Engineering substrate acceptance of Resveratrol *O*-Methyltransferase from *Vitis vinifera* for the selective synthesis of *O*-methyl protected biobased hydroxystyrenes

Kamela Myrtollari,[a, b, c] Andrea M. Chánique,[a, d] Daniel Kracher,[a, e] Daniela P. Herrera,[e] Joaquin Gutierrez-Benavente,[f] Andreas Schüller,[f, g] * Robert Kourist*[a, c, e]

[a] Graz University of Technology, Institute of Molecular Biotechnology, Petersgasse 14, 8010 Graz, Austria

[b] Henkel AG & Co. KGaA, Adhesive Research, Henkelstr. 67, 40191 Düsseldorf, Germany

[c] acib – Austrian Centre of Industrial Biotechnology Petersgasse 14, 8010 Graz, Austria

[d] Kura Biotech, Av. Gramado Interior 1410, Parcela 20, Puerto Varas, Chile

[e] BioTechMed-Graz Mozartgasse 12/II, 8010 Graz, Austria

[f] School of Biological Sciences, Pontificia Universidad Católica de Chile, Av. Libertador General Bernardo O'Higgins 340, Santiago, 8331150 Chile

[g] Institute for Biological and Medical Engineering, Pontificia Universidad Católica de Chile, Vicuña Mackenna 4860, Santiago, 7820244 Chile

Abstract

Enzymatic decarboxylation of phenolic acids enables the production of biobased phenolic styrenes under mild reaction conditions. However, the free *para*-phenolic group can lead to undesirable side products during polymerization, giving protection of the free phenolic OH group critical importance for the application in adhesives. Here we present a one-pot two-step cascade reaction, in which phenolic acid decarboxylase from *Bacillus subtilis* (*Bs*PAD) catalyzes the decarboxylation of coumaric acid, caffeic acid, ferulic acid, and sinapic acid, followed by *O*-methylation of the intermediate phenolic styrenes by resveratrol *O*-methyltransferase from *Vitis vinifera* (*Vv*ROMT). The reaction sequence avoids the isolation and purification of the reactive intermediate phenolic styrenes. The *O*-methyltransferase shows selectivity towards the phenolic styrenes. Characterization of a set of variants with amino acid substitution in the active-site cavity led to the identification of *Vv*ROMT L117F/F311W which did not show any activity towards the four phenolic acids. This avoids undesired *O*-methylation of the starting material, which is not desirable since the decarboxylase does not convert the formed *p*-methoxyphenolic acids. Furthermore, variation of amino acids in the active site led to the identification of mutants with improved activity for all four phenolic styrenes. The results constitute an important step towards the synthesis of biomass-derived methoxy styrene derivatives whose photopolymerization yields polymers with outstanding adhesion properties.

Introduction

The development of innovative, high-performance polymer materials requires monomers with unique functional groups that can promote their facile and effective polymerization. The use of functional phenolic styrene derivatives as polymer precursors has gained considerable attention because they can provide access to novel polymers with varied properties based on their functional groups.[1–5] In addition, they derive from naturally occurring hydroxycinnamic acids **1** and are thus potentially renewable building blocks for polymers and materials.[6] These acids are natural phenolic compounds that can be found in almost every plant. High concentrations of *p*-coumaric (**1a**), caffeic (**1b**), ferulic (**1c**) and sinapic acid (**1d**) can be found in berries,[7] coffee,[8] rice bran,[9] and oilseed crops,[10] respectively. While their concentrations in plants typically range from a few grams per kilogram of source material, they can also derive from highly abundant natural resources such as lignin, which is the second most abundant natural resource after cellulose.[11] A prominent example of the current utilization of phenolic acid is the production of vanillin from ferulic acid.[12] In the last years, biobased hydroxycinnamic acids have been receiving increasing interest as monomers for the manufacture of polymers. However, the steric hindrance around the substituted vinyl group is an obstacle to homopolymerization.[6] Even though they can be copolymerized with less bulky monomers, their content in the produced copolymers is still very low due to the same reason.[13,14] Condensation polymerization is an alternative but leads to the loss of hydroxy groups.[15–17] While the direct polymerization of the biobased hydroxycinnamic acids is of limited efficiency, their decarboxylation gives rise to phenolic styrene derivatives **2**.[18–20] Due to the electron-rich nature of their double bond, they can undergo polymerization via various mechanisms based on the functionality of the phenolic styrene derivative.[21–25] The diversity of the different bio-based phenolic acids allows achieving different properties of the final product in order to meet specific demands. For instance, 4-vinylphenol (**2a**) derived from *p*-coumaric acid is used in polymer chemistry for the production of photoresists, adhesives and epoxy-curing agents.[26–28] The decarboxylation product of caffeic acid, 4-vinylcatechol (**2b)**, is a key monomer for adhesive materials inspired by mussel adhesive protein.[2,29] Unfortunately, the hydroxy group is prone to induce side reactions, complicating the direct polymerization of these functional styrene derivatives.[30] This complicates their isolation, storage, and polymerization.[31] Furthermore, achieving controlled polymerization of phenolic styrenes is challenging. It requires demanding reaction conditions and the use of additives and chain-transfer agents, which limit their potential for technical application.[23,31,32] The tendency of phenolic styrenes to undergo spontaneous polymerization and side reactions complicate downstream processing.

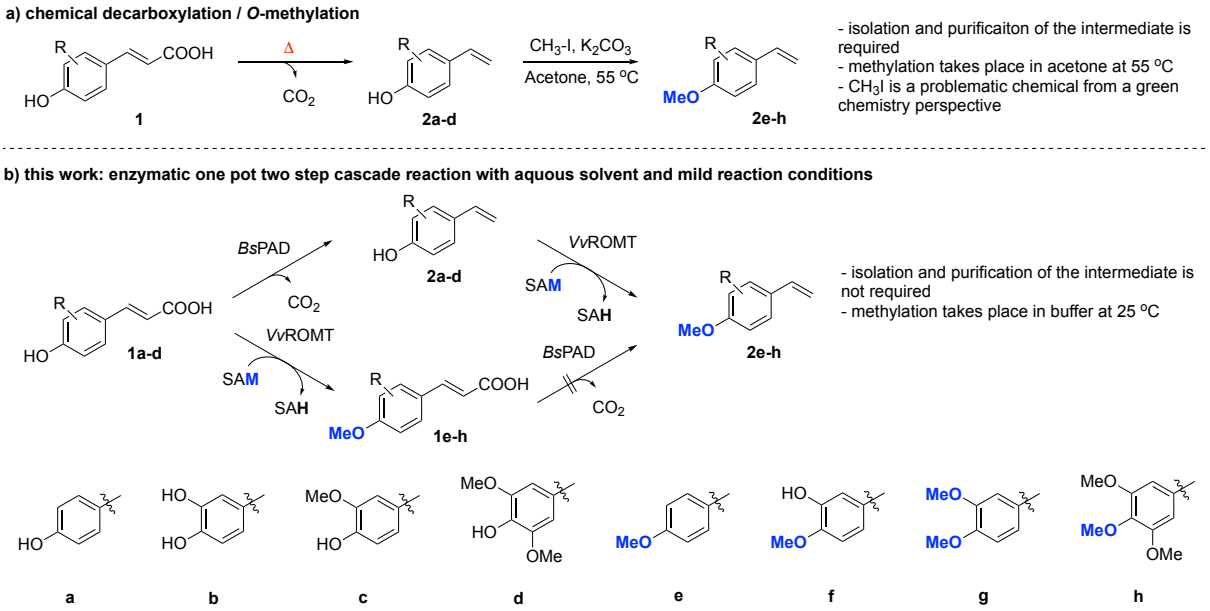

Scheme 1: a) Chemical preparation to produce substituted *para*- or *meta*-methoxystyrenes **2e-h** as protected biobased monomers of methoxy polystyrenes;[22,33] b) One-pot two-step reaction sequence for the decarboxylation of phenolic acids (**1a-d**) by phenolic acid decarboxylase from *Bacillus subtilis* (*Bs*PAD) and methylation of intermediate hydroxystyrene derivatives (**2a-d**) catalyzed by resveratrol *O*-methyltransferase from *Vitis vinifera* (*Vv*ROMT). *S*-Adenosyl-L-methionine (SAM) is provided as a methyl donor and SAH (*S*-adenosyl-L-homocysteine) is produced after the donation of the methyl group.

In most cases, *in situ* protection of the phenol group is required to maintain control over the polymerization while offering a more robust polymerization pathway. This has spurred an interest in the combination of decarboxylation with reactions for the protection of the phenolic group. Takeshima *et al.* reported the facile and scalable one-pot synthesis of bio-based *O*-protected phenolic styrenes via chemical decarboxylation of **1** followed by their direct protection via silylation or acetylation.[22] Recently, Petermeier *et al.* demonstrated that also enzymatic decarboxylation can be combined with chemical acetylation.[19] Acetylation and silylation of **2** facilitate controlled radical or anionic polymerization.[6,22,24] Modification of the functional group can alter the type of the polymerization mechanism and the properties of the final product. Acetylated or silylated monomers are limited to radical polymerization mechanisms. In contrast, methoxy styrenes can undergo cationic photopolymerization to yield polymers with great adhesion properties.[4,5,34] For example, 4-methoxystyrene is used in radical and cationic polymerizations to produce polymers used in coatings, adhesives, and optical devices.[4,5] 3,4-Dimethoxystyrene is also used in polymer chemistry for the preparation of underwater adhesives.[35]

Decarboxylation of phenolic acids at elevated temperatures is energy-consuming and prone to lead to undesired side-reactivities.[22] Moreover, methylation by methyl iodine is highly problematic from a green chemistry perspective.[33] In contrast, enzymatic decarboxylation and methylation reactions proceed under very mild reaction conditions.[36,37] For this, phenolic acid decarboxylase from *Bacillus subtilis* (*Bs*PAD) has shown high activity and stability.[18–20] As the decarboxylation of **1a-d** proceeds in an aqueous system, enzymatic *O*-methylation can follow under the same conditions without the requirement of the isolation and purification of the intermediates **2a-d** (Scheme 1). Cofactor-free phenolic acid decarboxylase employs an electron-relay mechanism comprised of the delocalized □-electron system and the essential *p*-hydroxy group on the substrate for the stabilization of the nascent negative charge upon loss of the carboxylate.[38,39] *O*-methylation of **1** would disrupt hydrogen bonds

between the *p*-hydroxy group and two catalytic Tyr residues, preventing decarboxylation of *p*-methoxy phenolic acids **1e-h**. Therefore, the order methylation-decarboxylation would not work with bacterial PAD. Decarboxylases accepting methoxy-cinnamic acids have been described but have much lower activity than *Bs*PAD.[40] For PAD, the order decarboxylation-methylation is therefore preferred (Scheme 1b). In view of a possible simultaneous mode of the cascade, we were interested in an *O*-methyl transferase (OMT) that would accept the hydrophobic phenolic styrenes **2a-d** as substrates, but not the hydrophilic acids **1a-d**. Plant OMTs are classified into three different types based on the protein sequence and structures.[41,42] Type I OMTs are cation-independent and active towards hydroxyl moieties of phenylpropanoids. Type II OMTs are cation-dependent and are mainly involved in the biosynthesis of lignin. Finally, type-III OMTs are mainly active towards carboxylic acids. For the methylation of catechol-like compounds type-I OMTs are mainly used such as OMT3 from *Sorghum bicolor* (*Sb*OMT3),[43] OMT1 from *Arabidopsis thaliana* (*At*OMT1)[44] and OMT from *Vitis vinifera* (*Vv*ROMT).[45] The latter stands out with its good activity towards hydroxylated stilbenes. In previous work, we were able to increase *Vv*ROMT mono- and di-methylation activity towards resveratrol by rational design of its active site.[46] We hypothesized that due to the high hydrophobicity of its active site, *Vv*ROMT would accept the highly hydrophobic phenolic styrenes **2** while showing less activity towards the polar phenolic acids **1**. The selection of *VvROMT* is further supported by the availability of active-site mutants from Herrara et al.[46] The predicted variants with amino acid substitutions in the hydrophobic active site cavity were based on molecular modeling and a comparative analysis of binding site residues. Investigation of a set of 7 variants revealed significant differences in the *O*-methylation of resveratrol and pinostilbene, respectively. In lieu of experimentally determined structures and anticipated difficulties in achieving accurate predictions on the effect of amino acid substitutions on the activity towards the small, hydrophobic **1a-d**, this set appeared to be a very promising basis for the identification of variants for their conversion.

Results and Discussion

Decarboxylation of coumaric acid **1a**, caffeic acid **1b**, ferulic acid **1c,** and sinapic acid **1d** catalyzed by cell-free extracts of PAD was performed in 500 mg-scale. For the successful decarboxylation of sinapic acid, the variant *Bs*PAD I85A was employed.[18] This mutant was created analogous to a mutant of *Bacillus pumilus* PAD and has increased activity towards *p*-hydroxycinnamic acids bearing two substituents in *meta*-position.[47] With all four phenolic acids investigated, the reactions proceeded quickly to completion as shown in Scheme 2, and the reaction mixture was immediately used for experiments on the *O*-methylation.

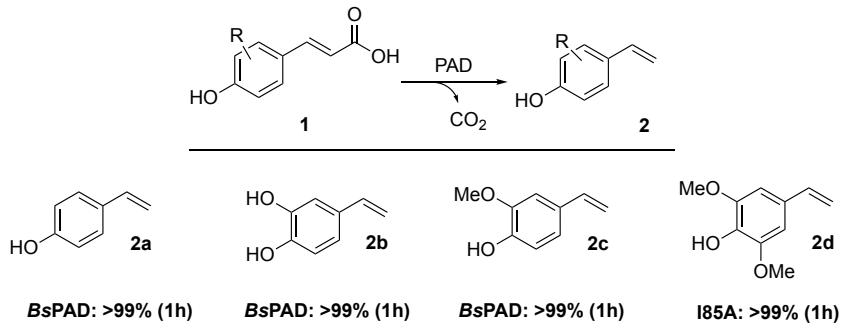

Scheme 2: PAD-catalyzed decarboxylation of bio-based hydroxycinnamic acids. Decarboxylation of substrates (10 mM) *p*-coumaric (**1a**), caffeic (**1b**) and ferulic acid (**1c**) was initiated by the wild type *Bs*PAD, while sinapic acid (**1d**) was converted by the cell-free extract of variant PAD I85A (100mg/mL). Reaction products were identified by GC-MS and verified with HPLC.

To clarify whether *Vv*ROMT would also convert the phenolic and catecholic hydroxy groups of the *p*-hydroxycinnamic acids **1a**-**d** we then investigated the methylation patter of *Vv*ROMT wild-type and a set of seven variants monitoring the formation of the *p*-methoxycinnamic acids **1e**-**h** (Scheme 1). The set included *Vv*ROMT wildtype (WT), *Vv*ROMT F311W (Mut1), *Vv*ROMT L117F/F311W (Mut2), *Vv*ROMT F318Y/A319N (Mut3), *Vv*ROMT L117F/F311W/T314L/F318V (Mut4), *Vv*ROMT F318R/A319N/F311W (Mut5), *Vv*ROMT L117F (Mut6), and *Vv*ROMT L117F/F311L/T314L/F318L (Mut7).

In previous work, some of the variants had moderately higher activity towards resveratrol, and much higher activity towards the intermediate pinostilbene compared to the wild-type, which resulted in a much higher overall activity in the two consecutive *O*-methylations leading from resveratrol to pterostilbene.[46] As expected, the activity of *Vv*ROMT and its variants towards the different *p*-hydroxycinnamic acids was very low. In biotransformations of *p*-coumaric acid **1a** and caffeic acid **1b** by wild-type *Vv*ROMT and the seven variants, neither substrate consumption nor product formation was observed (Figure 1). For **1b**, this means that neither of the two catecholic hydroxy groups could be methylated.

While wild-type *Vv*ROMT did not convert **1c**, variants Mut4 and Mut6 showed low activity after 24 h (**Fehler! Verweisquelle konnte nicht gefunden werden.**). Interestingly, sinapic acid **1d** having only one additional methoxy group was converted with much higher activity than **1c**.

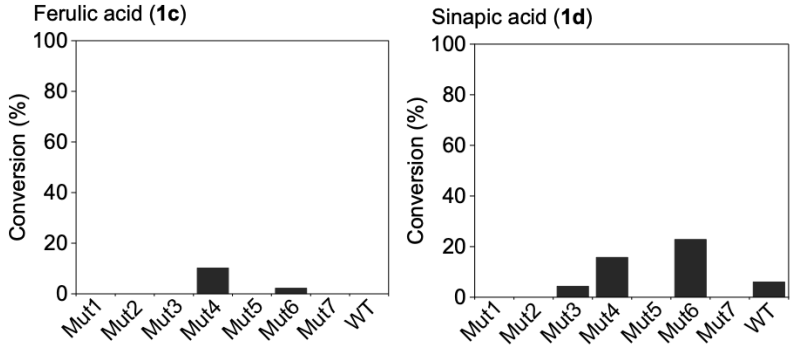

Figure 1: *O*-methylation of the 4-OH group of ferulic acid 1c and sinapic acid 1d by *Vv*ROMT and variants. 1a and 1b were not converted. Reaction conditions: 1 mM phenolic acid, 5 µM of the enzyme, 2 mM SAM in 100 mM Tris-HCl, pH 7.5 (containing 5 mM $MgCl_2$ and 0.5 mM DTT) at 25°C and 750 rpm for 24 h. Conversion was determined by HPLC **(n=3)**.

Mut6 exhibited the highest activity and achieved 22% conversion after 24h. In summary, the phenolic acids **1a-d** are generally poorly accepted by *Vv*ROMT and its mutants. For each of the phenolic acids, there are variants available with selectivity for the methylation of **2a-d** without undesired conversion of **1a-d**. Yet, even the methylation of small amounts of **1a-d** will prevent enzymatic decarboxylation, leading to the accumulation of the intermediate **1e-f**. Therefore, a sequential mode of decarboxylation and methylation was chosen as a practical approach mode for the envisioned reaction sequence.

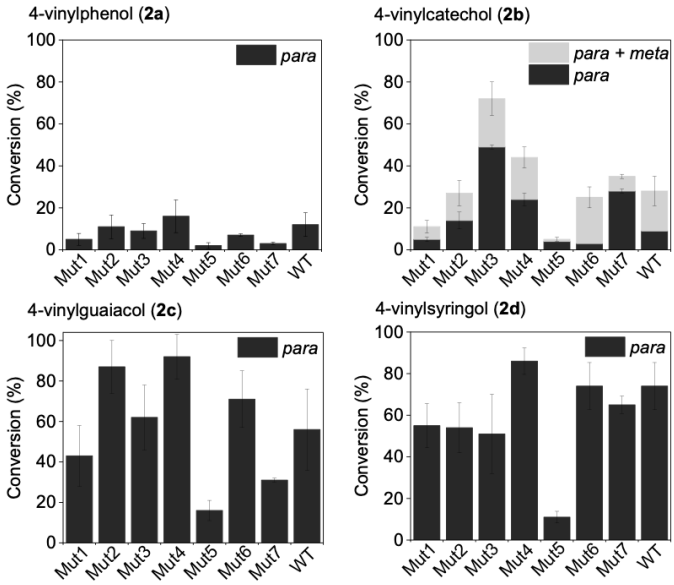

Figure 2: Methylation by *Vv*ROMT and its mutants of different phenolic styrenes (**2a-2d**) obtained from the enzymatic decarboxylation of the hydroxycinnamic acids is reported. Reaction conditions: 1 mM of styrene derivatives, 5 µM of the enzyme, 2 mM SAM in 100 mM Tris-HCl, pH 7.5 (containing 5 mM $MgCl_2$ and 0.5 mM DTT) at 25°C and 750 rpm for 24h. Values represent an average of 2 replicates. The reaction was monitored by HPLC (n=3).

The investigation of the *O*-methylation of *para*-hydroxy groups of the phenolic styrenes arising from the enzymatic decarboxylation focused on the effect of the different substituents on the aromatic ring on the activity of the mutants. Furthermore, we were interested to which extent the variants would be regioselective towards the two catecholic hydroxy groups of **2b**. After the completion of the enzymatic decarboxylation (Scheme 2), an appropriate volume of this reaction solution with the produced functional styrene was added to a new vial containing the methylation buffer and the corresponding methyltransferase without workup or purification of the intermediate. **Fehler! Verweisquelle konnte nicht gefunden werden.** shows the comparison of *Vv*ROMT wildtype and the seven variants. As expected, the activity was higher towards the more hydrophobic phenolic styrenes **2** than toward the corresponding phenolic acids **1**. While **1a** was not accepted by any of the variants, **2a** was converted, albeit with relatively low conversions.

The activity of the wild-type and three of the mutants towards **2b** was also lower compared to the activity towards **2c** and **2d**, showing that the small and relatively polar phenolic styrenes **2a** and **2b** are poor substrates for the enzyme. In particular, mutants Mut4, Mut7, and especially Mut3 showed much higher conversion of **2b**, underlining that amino acid substitutions in the hydrophobic active-site pocket strongly influence the activity of *Vv*ROMT towards small hydrophobic substrates. Substrate **2b** differs from the others as it offers two hydroxy groups whose methylation requires very different binding poses in the

narrow active site cavity. Interestingly, *Vv*ROMT and all investigated variants showed strict selectivity for the *O*-methylation of the *meta*-hydroxy group (Scheme 3). This striking regioselectivity resembles the selectivity of *Vv*ROMT for the *meta*-hydroxy groups of resveratrol and pinostilbene, respectively, whereas the *para-hydroxy groups* of both were not converted.[46] *O*-methyl transferases are often regioselective towards catecholic substrates.[37] For instance, isoeugenol *O*-methyltransferase from *Clarkia breweri* was highly regioselective for the methylation of the 3'-OH group of the flavonoids eriodictyol, luteolin, and quercetin.[36] *O*-methylation of **2b** forms vinyl guaiacol **2c**, which is itself a substrate of the enzyme. This allows direct conversion of caffeic acid via coupled decarboxylation and the two *O*-methylation steps directly into *para*-, *meta*-dimethoxystyrene **2g**.

Overall, **2b**, **2c,** and **2d** were converted by all variants with good activity, achieving conversions up to 90%. Interestingly, the *O*-methylation of the *para*-hydroxy groups of the methoxy-substituted substrates vinyl guaiacol **2c** and canolol (4-vinyl syringol) **2d** proceeded with much higher activity compared to **2a** and **2b**, leading up to 90% conversion. The presence of methoxy groups in **2d** and **2c** could favor the stabilization of the substrate in the pocket.

Table 1. Conversion of phenolic substrates by *Vv*ROMT and variants *Vv*ROMT Mut 1-7.

Entry	Enzyme	Nr.	Conversion									
			resv.[1,2]	pinost.[1]	1a[3]	1b	1c	1d	2a	2b[4]	2c	2d
			(%)									
1	*Vv*ROMT	wt	44.2	88.8	0	0	0	6.0	12.4	28.0	56.2	74.2
2	*Vv*ROMT F311W	Mut1	44.9	30.0	0	0	0	0	5.2	11.2	43.3	55.2
3	*Vv*ROMT L117F/F311W	Mut2	73.6	19.2	0	0	0	0	11.2	26.8	87.0	54.0
4	*Vv*ROMT F318Y/A319N	Mut3	17.4	19	0	0	0	4.3	9.0	72.0	62.3	51.2
5	*Vv*ROMT L117F/F311W/T314L/F318V	Mut4	37.0	4.8	0	0	10.2	15.7	16.3	43.8	92.2	86.1
6	*Vv*ROMT F318R/A319N/F311W	Mut5	0	0	0	0	0	0	2.5	4.6	16.5	11.1
7	*Vv*ROMT L117F	Mut6	70.6	89.9	0	0	2.3	22.8	7.3	24.8	71.4	74.2
8	*Vv*ROMT L117F/F311L/T314L/F318L	Mut7	11.6	4.3	0	0	0	0	3.4	34.7	31.6	65.1

[1] taken from ref. 46; [2] formation of pinostilbene and pterostilbene (Ref 46); [3] *para*- and *meta*-methylation; [4] determined by HPLC after 24 hours.

Consideration on substrate acceptance of *Vv*ROMT

The three-dimensional structure of *Vv*ROMT was previously modeled in a closed, catalytically competent dimeric conformation, containing the substrate and the co-substrate *S*-adenosylmethionine (SAM).[46] The substrate-binding site of *Vv*ROMT is composed of hydrophobic residues. Molecular docking revealed that in the catalytically competent binding mode of resveratrol, the molecule is oriented with its 3-OH group towards the sulfonium group of SAM. Specific residues such as F24, F167, F311, and F318 stabilize resveratrol through aromatic interactions, while other hydrophobic interactions involve L117, M121, M171, W258, and M315. Among these, F311 was identified as a critical residue for substrate stabilization and catalytic function, as confirmed by both *in silico* and experimental analyses. The possible binding of hydroxystyrenes is exemplified by positioning **2d** in the *Vv*ROMT model (Figure

3a). A structural prediction from AlphaFold 3 revealed differences in the helical region when compared to the model, shifting active site residues. This highlights the limitations of *in silico* approaches without the support of experimental data. After energy minimization, **2d** was positioned in the active site of the model in the *para* position with the OH group oriented towards the sulfonium group of SAM (3.2 Å distance) and was also in close proximity to the catalytic H261 (3.5 Å). Interestingly, the predicted orientation of **2d** in the *Vv*ROMT binding site was rotated by 60 degrees with respect to the predicted binding mode of resveratrol, to accommodate for methylation in the *para* position. The orientation of **2d** resembles that of other type I OMT substrates that are *para* methylated, such as isoeugenol and sinapyl alcohol (*Clarkia breweri* (iso)eugenol *O*-methyltransferase; PDB codes 3reo, 5cvu), and isoformononetin (*Medicago sativa* isoflavone-7-*O*-methyltransferase 8; PDB code 1fp2).[48] However, our predicted binding mode of the substrates **2b** and **2f** with methylation in *meta* position resembles that of resveratrol in our *Vv*ROMT model, and the *meta*-methoxy products sinapaldehyde and coniferaldehyde in complex with *Lolium perenne* caffeic acid *O*-methyltransferase (PBD codes 3p9i, 3p9k).[49]

Table 1 summarizes the activity of *Vv*ROMT and the seven variants with active site amino acid substitutions in the conversion of the phenolic acids and phenolic styrenes in comparison to the conversion of two hydroxystilbenes. In the conversion of **1a-d** and **2a-d** by *Vv*ROMT, two main trends were observed: *Vv*ROMT converts the phenolic styrenes much faster than the phenolic acids **1**. Within the former group of substrates, the activity towards the larger **2c** and **2d** is higher than towards the smaller **2a** and **2b**.

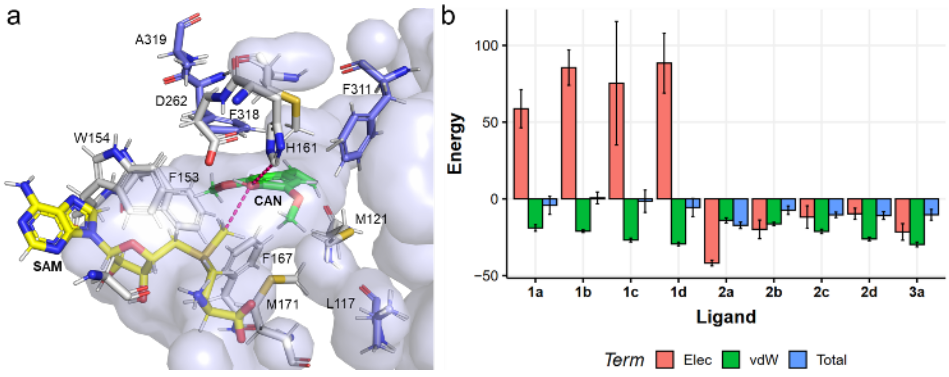

Figure 3: a, Model of *Vv*ROMT showing the active site bound to **2d** (canolol, green). Residues shown in blue were targeted by directed mutagenesis. **b,** binding energy divided into an electrostatic component (Elec) and a van der Waals component (vdW).

The discrimination between **1** and **2** can be attributed to differences in their compatibility with the active site. The substrate binding site is highly hydrophobic and does provide little polar surface area for the formation of polar interactions, in particular hydrogen bonds. In the *Vv*ROMT structural model, 89% of the surface area of the substrate binding site buried by resveratrol is hydrophobic, as calculated by the tool dr_sasa.[50] Analysis of the electrostatic (Elec) and van der Waals (vdW) energy terms of the binding free energy estimated by the MM-PBSA method in 5 ns molecular dynamics simulations revealed a positive electrostatic energy for the deprotonated acids **1a-d**, while negative Elec values were observed for all other ligands (Figure 3b). The vdW-energy was negative for all ligands and the total free binding energy was close to zero for the deprotonated acid and more negative for all other ligands (Figure 3b).

Therefore, interactions with the non-polar styrene group are strongly favored, leading to the observed discrimination against the polar carboxy group. The capacity of variants Mut1, Mut2, and Mut5 to fully discriminate between **1** and **2** is significant as it allows the combination of decarboxylation and *O*-methylation in a one-pot reaction without undesired conversion of the phenolic acids.

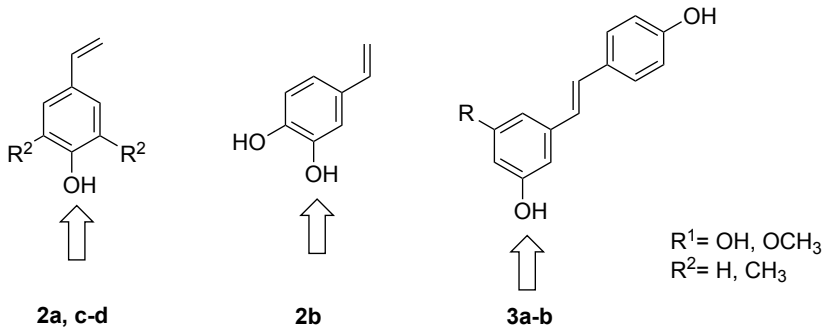

Scheme 3: The substrates **2a-d**, resveratrol **3a** and pinostilbene **3b** must be accommodated in different poses in the active site cavity of *Vv*ROMT, depending on the position of the hydroxy group to be methylated (*meta/para*). The hydroxy groups attacking the reactive methyl group of SAM are highlighted with an arrow.

The higher activity of *Vv*ROMT and its variants towards the larger phenolic styrenes can be attributed to different reasons. *Vv*ROMT wildtype and the seven variants thereof show striking differences in substrate acceptance (Scheme 3). The effects of the mutations differ between the two stilbenes, the two larger **2c** and **2d** and the catecholic **2b**. These three groups constitute very different substrates for the enzyme. Both stilbenes have the methylated hydroxy group in *meta*-position. While the para-hydroxy group of **2c** and **2d** attacks the reactive methyl group of SAM, **2b** is methylated first in *meta*-position. The double mutant Mut3 is the most active variant in the methylation of **2b**, but converts resveratrol and pinostilbene poorly and has similar activity to the wildtype towards **2c** and **2d**. Both, **2c** and **2d** have a larger hydrophobic surface, which can possibly facilitate the accommodation of the substrate in the active site. Furthermore, the electron-pushing effect of the methoxy groups on the aromatic ring increases the nucleophilicity in the attack on the reactive methyl group of *S*-adenosylmethionine (SAM). These two effects appear to be more important than the steric hindrance caused by the additional methoxy groups. Mut2 introduces two larger aromatic residues into the active site in close proximity to the phenolic or catecholic ring, and the catalytic H161. The quadruple mutant Mut4 is the most active towards **2c** and **2d** and also very active towards **2b**. This variant stands out in its relatively high activity towards **1c** and **1d**. In contrast, the activity towards resveratrol is lower than that of the wild-type enzyme, and the activity towards pinostilbene is very low. Mut6 has the single substitution L117F, Mut1 the substitution F311W, and the double variant Mut2 combines both (L117F/F311W). While Mut6 has the highest activities towards resveratrol and shows good activity towards the phenolic acids **1c** and **1d**, it is neutral towards the phenolic styrenes. The triple variant Mut5 has an arginine in the hydrophobic active site. This variant has consistently low activity towards all substrates. Without experimentally determined structural information, accurate explanations of the effect of the amino acid substitutions in the hydrophobic active site cavity on the O-transmethylation activity are difficult. *Vv*ROMT is a dimer, where amino acids from one monomer contribute to the active site of the other. This constellation makes accurate predictions of substrate binding and -targeting exceedingly challenging. Our results highlight

the advantages of screening a small but high-quality enzyme library with verified activities. Especially in the case of enzymes with large, hydrophobic binding sites, precise predictions of enzyme-substrate interactions are difficult.[51] Estimating the binding free energy with the MM-PBSA method correlated poorly with our experimental results. The library investigated here contains for each of the four substrates **2a-d** at least one variant with the desired properties for the application in the cascade reaction shown in Scheme 1. These are the suppression of *O*-methylation of the phenolic acids **1** and higher activity towards the intermediate phenolic styrenes **2**.

While our results show the feasibility of the enzyme cascade, the supply of the co-substrate SAM is a limitation. Stoichiometric addition is not economically feasible for the synthesis of monomers. In the last years, different multi-enzyme cascade reactions have been developed for the regeneration of SAM or its *in situ* formation from inexpensive precursors. [52–55] Halide methyltransferases transfer methyl groups from methyl iodide to SAH [53,56] and their activity could be improved by directed enzyme evolution. [54] The enzymatic approach has the advantage that the problematic methyl iodide can be applied in small concentrations. SAM is produced from L-methionine and ATP. This was exploited in a multi-enzyme cascade of six enzymatic steps that couples regeneration of SAM to enzymatic polyphosphate degradation. [52] Similarly, the bacterial metabolism can be used to supply SAM in whole-cell biocatalysts.[56] Recently, the intracellular supply of SAM was improved by betaine as the methyl source by introducing a betaine-homocysteine methyltransferase and coupling it to *S*-adenosyl-L-homocysteine (SAH) hydrolysis pathways, underlining the feasibility to supply SAM in whole-cell biocatalysts.[56] The rapid progress in the regeneration of SAM raises the expectation that the improvements needed for the synthesis of biobased chemicals can be achieved in the near future.

Conclusion

Preparation and *in-situ* protection of phenolic styrenes was successfully implemented via a biocatalytic reaction sequence using phenolic acid decarboxylase from *Bacillus subtilis* followed by the direct methylation of the intermediates in the presence of resveratrol *O*-methyltransferase from *Vitis vinifera*. The reaction conditions used are much milder than those reported for the chemical decarboxylation and methylation reactions, respectively. The one-pot two-step reaction avoids workup and purification problems caused by the instability of the decarboxylation products. Finally, the cascade yields *p*-methylated functional styrenes which are more stable and are amendable to various cationic photopolymerizations. Overall, this approach serves as a promising proof of concept, demonstrating robust efficacy with specific substrates; however, further optimization is required to achieve better conversion for the less reactive styrenes.

Experimental Section

Materials

S-adenosyl-L-homocysteine, *S*-adenosyl-L-methionine, and all other chemicals were purchased from Sigma-Aldrich, TCI, and Alfa Aesar and were of analytical grade or higher purity and used as received. The resveratrol *O*-methyltransferase (ROMT) from *Vitis vinifera* was kindly provided by Dr. Loreto Parra, Assistant Professor at the Department of Chemical Engineering and Bioprocesses of the Pontifical Catholic University of Chile.

Expression and purification of *Bs*PAD and variant I85A

Synthetic genes encoding the enzymes were purchased from Twist Biosciences (South San Francisco, USA), transformed, checked for correct insertion by sequencing, and expressed in *E. coli* BL21 (DE3) strains.[18] Transformants were inoculated in 5 mL LB medium (1% peptone, 0.5% yeast extract, 1% NaCl) containing 5 μg mL^{-1} kanamycin and grown at 37 ºC and 130 rpm overnight. The cultures were used to inoculate 400 mL of TB-Kan medium (40 μg mL^{-1}). The cells were grown at 37 ºC and 130 rpm until an OD_{600} of 0.5−0.7 was reached. Expression was started by induction with IPTG (0.1 mM) followed by incubation at 20 °C and 120 rpm for 20−24 h. The cells were harvested by centrifugation (15 min, 4500 rpm, 4 °C). The resulting pellet was washed with 50 mM potassium phosphate buffer pH 6 and stored at −20 °C. The enzymes were purified as described earlier.[18]

Expression and purification of *Vv*ROMT and mutants

An *E. coli* strain BL21 (DE3) culture, containing the pET25-GB1-ROMT vector, was grown in Terrific Broth (1.2% tryptone, 2.4% yeast extract, 0.3% glycerol, and 100 mM phosphate buffer, pH 7.4) supplemented with kanamycin at 50 μg mL^{-1}. Then, cells were cultivated at 37 ºC at 150 rpm until an OD_{600} 0.6–0.8 was reached. *Vv*ROMT expression was induced by adding IPTG at a final concentration of 0.5 mM. After 17 h of incubation at 28 ºC and 150 rpm, cells were harvested by centrifugation (4000 rpm, 4 ºC for 30 min) and resuspended in buffer A (20 mM Tris-HCl, pH 7.5, 500 mM NaCl, 10% glycerol, 20 mM imidazole) plus 10 mM DTT, 1 mM PMSF, and 10 U DNAase. Lysis was performed by sonication for 7 min (7 seg ON 15 seg OFF) on ice, with a Q125 Sonicator (QSonica, Newton, CT, USA). Lysate was centrifuged (13,000 rpm, 30 min at 4 ºC), and the clarified supernatant was passed through a sterile 0.22 μM MCE membrane BIOFIL syringe filter.

*Vv*ROMT purification was carried out through immobilized metal affinity chromatography (IMAC), using a HisTrap FF column (GE Healthcare Biosciences, Pittsburgh, PA, USA) according to the manufacturer's instructions. The clarified extract was loaded onto the column, which was preconditioned with buffer A, and after 10-bed column washes, the fusion protein was eluted with elution buffer (20 mM Tris-HCl, pH 7.5, 500 mM NaCl, 10% glycerol) using a four-step imidazole gradient (50, 100, 180, and 250 mM) or a linear gradient. The selected fractions were pooled according to visualization by SDS-PAGE or by absorbance at 280 nm. Buffer exchange using Amicon Ultra-15 Centrifugal Filter Units (NMWL 30 kDa; Merck Millipore) was performed twice with buffer A, without imidazole. GB1-ROMT

fusion protein was subjected to proteolytic removal of the N-terminal GB1 protein using a His-tagged TEV protease followed by one-step final purification using IMAC, as mentioned above.

Protein concentrations were determined with the Bradford assay (Biorad, Hercules, CA, USA) using bovine serum albumin as a calibration standard. Purification of ROMT variants was conducted in the same manner. Proteins were used immediately for enzymatic reactions or stored at −80 ºC with 20% glycerol.

Methylation of phenolic acids

Initially, the reaction buffer (100 mM Tris-HCl, 5 mM $MgCl_2$, 0.5 mM DTT, pH 7.5) was added followed by the addition of 2 mM SAM and 5 µM of the enzyme. The reaction mixture was incubated in a thermomixer at 25 °C, 750 rpm. The respective substrate (**1a-d**) in a stock solution of DMSO (200 mM) was added in the appropriate volume to reach the final substrate concentration of 1 mM. Methylation of hydroxycinnamic acids was monitored by HPLC. However, confirmation of the methylation products through HPLC analysis was not possible due to the absence of authentic standards. The appearance of a second peak other than the peak of the confirmed starting material is assigned to the corresponding methylation product.

Reaction sequence: Enzyme Activity

Decarboxylation of caffeic acid, *p*-coumaric acid, ferulic acid, and sinapic acid for the synthesis of **2a-d** was achieved according to the literature.[18] All reactions were performed on a 1 mL scale in 1.5 mL reaction tubes. The respective substrate pre-dissolved in DMSO (200 mM stock) was mixed with the reaction buffer (50 mM potassium phosphate buffer, pH 6), to reach a final concentration of 10 mM. The reaction was initiated after the addition of the respective amount of the lyophilized enzyme (typically 0.4 mg mL^{-1}) or the CFE of variant I85A (100 mg mL^{-1}) in the case of **2d** while incubated at 30 °C with 600 rpm in a Thermomixer. When the full conversion was detected by TLC (cyclohexane/ ethyl acetate= 1/1, CAM or UV), samples of 150 µL were taken and extracted with MTBE (2×100µL). The combined organic layers were dried over Na_2SO_4 and after mixing and centrifugation to allow precipitation of Na_2SO_4, the supernatant could be used for GC-MS analysis. For HPLC analysis, samples of 100 µL were taken and quenched by the addition of 150 µL ACN (containing 400 mM HCl). After centrifugation to allow enzyme precipitation, the supernatant was used for HPLC measurements. All substrates were fully converted after 1 h.

The aforementioned reaction solution was used as stock for the methylation reaction. The appropriate volume of that solution was added to a new vial containing the buffer for the methylation (100 mM Tris-HCl, pH 7.5, 5 mM $MgCl_2$, 0.5 mM DTT) to reach a final substrate concentration of 1 mM followed by the addition of 5 µM of the purified enzyme and 2 mM SAM. Reactions were incubated at 25 °C with 750 rpm in a Thermomixer. The final reaction volume was 150 µL. Samples were taken after 0 and 24 h and an equal volume of acetonitrile (100 mM HCl) was added to quench the reaction. The samples were centrifuged at full speed for 60 min and then 200 µL supernatant was transferred to microwells before HPLC analysis. The wavelength chosen for the detection of the methylated products is 305 nm.

The identities of meta-, para- and double-methylated products were confirmed by comparison with chromatographic elution times of commercial standards.

High-Performance Liquid Chromatography

All HPLC analyses were performed on an Agilent Technologies 1100 Series with an autosampler and DAD detector together with a reversed-phase Nucleodur C18 Pyramid column (5 µm, 250 × 4.6 mm, Macherey Nagel). The mobile phase used was acetonitrile/water (0.01% acetic acid) at different concentrations based on the elution products. All methods and parameters can be found in the supporting (Table S2). The detection wavelength was 305 nm. Products were confirmed with GC-MS analysis. All reactions were performed in duplicates.

Gas Chromatography–Mass Spectrometry

GC–MS was used to confirm the formation of the desired product. All measurements were performed on a Shimadzu GCMS-QP2010 SE instrument equipped with an AOC-20i/s autosampler and injector unit together with a Zebron ZB-5MSi capillary column (30 m × 0.25 mm x 0.25 µm, Phenomenex). For GC–MS analyses, the reaction buffer was extracted using the same volume of dichloromethane. Phases were separated and the organic layer was dried over anhydrous $MgSO_4$. A 1:10 dilution was used for measurements.

Binding free energy calculations

Ligands were modeled in the substrate binding site of our *Vv*ROMT structural model[46] utilizing resveratrol as a reference. Binding free energy was estimated with the Molecular Mechanics/Poisson Boltzmann Surface Area (MM-PBSA) method through an automated in-house pipeline inspired by the webserver farPPI[57] with calculations performed using Amber16's mm_pbsa.pl script and AmberTools20.[58,59] The pipeline was setup to prepare the cosubstrate SAM and the ligands using antechamber and tleap to assign partial charges with the AM1-BCC method and to prepare the protein with pdb4amber and tleap.[60] A negative charge was assumed for the deprotonated acids **1a-d**. The protein was parameterized with ff19SB[61] and the small molecules with the general Amber force field (GAFF, version 2.1).[62] The workflow also handled the system setup, solvating it in a periodic truncated octahedron with and OPC water model, extending at least 10 Å from the solute and neutralizing by adding sodium ions. PARSE radii were applied. The system was minimized as described by Wang *et al.*[57] with a non-bonded interactions cut-off of 9 Å and the particle mesh Ewald algorithm for long-ranged interactions, followed by heating to 300 K for 500 ps using a Langevin thermostat. Then, the system underwent density adjustment for 500ps and a 2ns equilibration at constant pressure. Finally, 5 ns of production simulations were carried out. 250 snapshots were extracted from the trajectory and processed by mm_pbsa.pl. This procedure was automatically repeated five times for each ligand.

Acknowledgements

This project has received funding from the European Union's Horizon 2020 research and innovation program under the Marie Skłodowska-Curie grant agreement no. 860414.

Keywords: decarboxylase • *O*-methyltransferase • polymer precursors • enzyme engineering • styrene derivatives

References

[1] J. Horsch, P. Wilke, M. Pretzler, M. Seuss, I. Melnyk, D. Remmler, A. Fery, A. Rompel, H. G. Börner, *Angew. Chem. - Int. Ed.* **2018**, *57*, 15728–15732.

[2] P. Kord Forooshani, B. P. Lee, *J. Polym. Sci. Part Polym. Chem.* **2017**, *55*, 9–33.

[3] M. Cadenaro, T. Maravic, A. Comba, A. Mazzoni, L. Fanfoni, T. Hilton, J. Ferracane, L. Breschi, *Dent. Mater.* **2019**, *35*, DOI 10.1016/j.dental.2018.11.012.

[4] A. J. Perkowski, W. You, D. A. Nicewicz, *J. Am. Chem. Soc.* **2015**, *137*, 7580–7583.

[5] L. Wang, Y. Xu, Q. Zuo, H. Dai, L. Huang, M. Zhang, Y. Zheng, C. Yu, S. Zhang, Y. Zhou, *Nat. Commun.* **2022**, *13*, 3621.

[6] H. Takeshima, K. Satoh, M. Kamigaito, *J. Polym. Sci. Part Polym. Chem.* **2019**, 91–100.

[7] H. R. El-Seedi, A. M. A. El-Said, S. A. M. Khalifa, U. Göransson, L. Bohlin, A.-K. Borg-Karlson, R. Verpoorte, *J. Agric. Food Chem.* **2012**, *60*, 10877–10895.

[8] M. R. Olthof, P. C. Hollman, M. B. Katan, *J. Nutr.* **2001**, *131*, 66–71.

[9] H. T. Truong, M. Do Van, L. Duc Huynh, L. Thi Nguyen, A. Do Tuan, T. Le Xuan Thanh, H. Duong Phuoc, N. Takenaka, K. Imamura, Y. Maeda, *Appl. Sci.* **2017**, *7*, 796.

[10] C. Chen, *Oxid. Med. Cell. Longev.* **2016**, *2016*, 1–10.

[11] M. Chen, Y. Li, F. Lu, J. S. Luterbacher, J. Ralph, *ACS Sustain. Chem. Eng.* **2023**, *11*, 10001–10017.

[12] T. Furuya, M. Miura, M. Kuroiwa, K. Kino, *New Biotechnol.* **2015**, *32*, 335–339.

[13] Y. Terao, K. Satoh, M. Kamigaito, *Biomacromolecules* **2019**, *20*, 192–203.

[14] F. Puoci, F. Iemma, M. Curcio, O. I. Parisi, G. Cirillo, U. G. Spizzirri, N. Picci, *J. Agric. Food Chem.* **2008**, *56*, 10646–10650.

[15] D. Ishii, H. Maeda, H. Hayashi, T. Mitani, N. Shinohara, K. Yoshioka, T. Watanabe, in *Green Polym. Chem. Biocatal. Mater. II*, American Chemical Society, **2013**, pp. 237–249.

[16] O. Kreye, S. Oelmann, M. A. R. Meier, *Macromol. Chem. Phys.* **2013**, *214*, 1452–1464.

[17] S. Wang, S. Tateyama, D. Kaneko, S. Ohki, T. Kaneko, *Polym. Degrad. Stab.* **2011**, *96*, 2048–2054.

[18] A. K. Schweiger, N. Ríos-Lombardía, C. K. Winkler, S. Schmidt, F. Morís, W. Kroutil, J. González-Sabín, R. Kourist, *ACS Sustain. Chem. Eng.* **2019**, *16364–1637*, 1–19.

[19] P. Petermeier, J. P. Bittner, S. Müller, E. Byström, S. Kara, *Green Chem.* **2022**, *24*, 6889–6899.

[20] K. Myrtollari, E. Calderini, D. Kracher, T. Schöngaßner, S. Galušić, A. Slavica, A. Taden, D. Mokos, A. Schrüfer, G. Wirnsberger, K. Gruber, B. Daniel, R. Kourist, *ACS Sustain. Chem. Eng.* **2024**, *12*, 3575–3584.

[21] M. Kato, *J. Photopolym. Sci. Technol.* **2008**, *21*, 711–717.

[22] H. Takeshima, K. Satoh, M. Kamigaito, *ACS Sustain. Chem. Eng.* **2018**, *6*, 13681–13686.

[23] H. Takeshima, K. Satoh, M. Kamigaito, *R-Cl/SnCl 4 /n-Bu 4 NCl-Induced Direct Living Cationic Polymerization of Naturally-Derived Unprotected 4-Vinylphenol, 4-Vinylguaiacol, and 4-Vinylcatechol in CH 3 CN*, **2019**.

[24] J. van Schijndel, D. Molendijk, K. van Beurden, L. A. Canalle, T. Noël, J. Meuldijk, *Eur. Polym. J.* **2020**, *125*, 109534.

[25] G. G. Barclay, C. J. Hawker, H. Ito, ‡ A Orellana, P. R. L. L. Malenfant, R. F. Sinta, A. Orellana, P. R. L. L. Malenfant, R. F. Sinta, ‡ A Orellana, P. R. L. L. Malenfant, R. F. Sinta, *Macromolecules* **1998**, *31*, 1024–1031.

[26] J. M. Nasrullah, S. Raja, K. Vijayakumaran, R. Dhamodharan, *J. Polym. Sci. Part Polym. Chem.* **2000**, *38*, 453–461.

[27] S. G. Prolongo, G. Prolongo, *J. Therm. Anal. Calorim.* **2007**, *87*, 259–268.

[28] S. Peshkova, K. Li, *Wood Fiber Sci.* **2003**, 41–48.

[29] H. M. Siebert, J. J. Wilker, *ACS Sustain. Chem. Eng.* **2019**, *7*, 13315–13323.

[30] R. H. Still, A. Whitehead, *Thermal Degradation of Polymers. XV. Vacuum Pyrolysis Studies on Poly(p-Methoxystyrene) and Poly (p-Hydroxystyrene)*, **1977**.

[31] M. Kaneko, T. Noguchi, N. Oka, *Process for Preparing Vinyl Phenol Polymers and Stabilized Compositions of Vinyl Phenol-Containing Polymerization Raw Material*, **1998**, EP0864590A2.

[32] K. Satoh, M. Kamigaito, M. Sawamoto, *Macromolecules* **2000**, *33*, 5405–5410.

[33] E. Rigo, C. Totée, V. Ladmiral, S. Caillol, P. Lacroix-Desmazes, *Molecules* **2024**, *29*, 2507.

[34] J. V. Crivello, M. Sangermano, *J. Polym. Sci. A Polym. Chem.* **2001**, *39*, 343–356.

[35] V. Y. Kong, W. Z. Xu, P. A. Charpentier, *Ind. Eng. Chem. Res.* **2023**, *62*, 7411–7419.

[36] Q. Tang, U. T. Bornscheuer, I. V. Pavlidis, *ChemCatChem* **2019**, *11*, 3227–3233.

[37] F. Subrizi, Y. Wang, B. Thair, D. Méndez-Sánchez, R. Roddan, M. Cárdenas-Fernández, J. Siegrist, M. Richter, J. N. Andexer, J. M. Ward, H. C. Hailes, *Angew. Chem. Int. Ed Engl.* **2021**, *60*, 18673–18679.

[38] A. Frank, W. Eborall, R. Hyde, S. Hart, J. P. Turkenburg, G. Grogan, *Catal. Sci. Technol.* **2012**, *2*, 1568–1574.

[39] H. Rodríguez, I. Angulo, B. L. De Rivas, N. Campillo, J. A. Páez, R. Muñoz, J. M. Mancheño, *Proteins Struct. Funct. Bioinforma.* **2010**, *78*, 1662–1676.

[40] K. A. P. Payne, M. D. White, K. Fisher, B. Khara, S. S. Bailey, D. Parker, N. J. W. Rattray, D. K. Trivedi, R. Goodacre, R. Beveridge, P. Barran, S. E. J. Rigby, N. S. Scrutton, S. Hay, D. Leys, *Nature* **2015**, *522*, 497–501.

[41] J. P. Noel, R. A. Dixon, E. Pichersky, C. Zubieta, J.-L. Ferrer, in *Recent Adv. Phytochem.* (Ed.: J.T. Romeo), Elsevier, **2003**, pp. 37–58.

[42] R. K. Ibrahim, A. Bruneau, B. Bantignies, *Plant Mol. Biol.* **1998**, *36*, 1–10.

[43] Y. J. Jeong, C. H. An, S. G. Woo, H. J. Jeong, Y.-M. Kim, S.-J. Park, B. D. Yoon, C. Y. Kim, *Enzyme Microb. Technol.* **2014**, *54*, 8–14.

[44] K. T. Heo, S.-Y. Kang, Y.-S. Hong, *Microb. Cell Factories* **2017**, *16*, 30.

[45] J. Lücker, S. Martens, S. T. Lund, *Phytochemistry* **2010**, *71*, 1474–1484.

[46] D. P. Herrera, A. M. Chánique, A. Martínez-Márquez, R. Bru-Martínez, R. Kourist, L. P. Parra, A. Schüller, *Int. J. Mol. Sci.* **2021**, *22*, DOI 10.3390/ijms22094345.

[47] K. L. Morley, S. Grosse, H. Leisch, P. C. K. Lau, *Green Chem.* **2013**, *15*, 3312–3317.

[48] C. Zubieta, X. Z. He, R. A. Dixon, J. P. Noel, *Nat. Struct. Biol.* **2001**, *8*, 271–279.

[49] G. V. Louie, M. E. Bowman, Y. Tu, A. Mouradov, G. Spangenberg, J. P. Noel, *Plant Cell* **2010**, *22*, 4114–4127.

[50] J. Ribeiro, C. Ríos-Vera, F. Melo, A. Schüller, *Bioinforma. Oxf. Engl.* **2019**, *35*, 3499–3501.

[51] M. Biler, R. M. Crean, A. K. Schweiger, R. Kourist, S. C. L. Kamerlin, *J. Am. Chem. Soc.* **2020**, *142*, 20216–20231.

[52] S. Mordhorst, J. Siegrist, M. Müller, M. Richter, J. N. Andexer, *Angew. Chem. - Int. Ed.* **2017**, *56*, 4037–4041.

[53] C. Liao, F. P. Seebeck, *Nat. Catal.* **2019**, *2*, 696–701.

[54] Q. Tang, C. W. Grathwol, A. S. Aslan‐Üzel, S. Wu, A. Link, I. V. Pavlidis, C. P. S. Badenhorst, U. T. Bornscheuer, *Angew. Chem. Int. Ed.* **2021**, *60*, 1524–1527.

[55] S. Mordhorst, J. N. Andexer, *Nat. Prod. Rep.* **2020**, *37*, 1316–1333.

[56] Q. Liu, B. Lin, Y. Tao, *Metab. Eng.* **2022**, *72*, 46–55.

[57] Z. Wang, X. Wang, Y. Li, T. Lei, E. Wang, D. Li, Y. Kang, F. Zhu, T. Hou, *Bioinforma. Oxf. Engl.* **2019**, *35*, 1777–1779.

[58] D.A. Case, H.M. Aktulga, K. Belfon, I.Y. Ben-Shalom, J.T. Berryman, S.R. Brozell, D.S. Cerutti, T.E. Cheatham, III, G.A. Cisneros, V.W.D. Cruzeiro, T.A. Darden, N. Forouzesh, M. Ghazimirsaeed, G. Giambaşu, T. Giese, M.K. Gilson, H. Gohlke, A.W. Goetz, J. Harris, Z. Huang, S. Izadi, S.A. Izmailov, K. Kasavajhala, M.C. Kaymak, A. Kovalenko, T. Kurtzman, T.S. Lee, P. Li, Z. Li, C. Lin, J. Liu, T. Luchko, R. Luo, M. Machado, M. Manathunga, K.M. Merz, Y. Miao, O. Mikhailovskii, G. Monard, H. Nguyen, K.A. O'Hearn, A. Onufriev, F. Pan, S. Pantano, A. Rahnamoun, D.R. Roe, A. Roitberg, C. Sagui, S. Schott-Verdugo, A. Shajan, J. Shen, C.L. Simmerling, N.R. Skrynnikov, J. Smith, J. Swails, R.C. Walker, J. Wang, J. Wang, X. Wu, Y. Wu, Y. Xiong, Y. Xue, D.M. York, C. Zhao, Q. Zhu, and P.A. Kollman, *Amber 2024*, University Of California, San Francisco, **2024**.

[59] D. A. Case, H. M. Aktulga, K. Belfon, D. S. Cerutti, G. A. Cisneros, V. W. D. Cruzeiro, N. Forouzesh, T. J. Giese, A. W. Götz, H. Gohlke, S. Izadi, K. Kasavajhala, M. C. Kaymak, E. King, T. Kurtzman, T.-S. Lee, P. Li, J. Liu, T. Luchko, R. Luo, M. Manathunga, M. R. Machado, H. M. Nguyen, K. A. O'Hearn, A. V. Onufriev, F. Pan, S. Pantano, R. Qi, A. Rahnamoun, A. Risheh, S. Schott-Verdugo, A. Shajan, J. Swails, J. Wang, H. Wei, X. Wu, Y. Wu, S. Zhang, S. Zhao, Q. Zhu, T. E. I. Cheatham, D. R. Roe, A. Roitberg, C. Simmerling, D. M. York, M. C. Nagan, K. M. Jr. Merz, *J. Chem. Inf. Model.* **2023**, *63*, 6183–6191.

[60] A. Jakalian, D. B. Jack, C. I. Bayly, *J. Comput. Chem.* **2002**, *23*, 1623–1641.

[61] C. Tian, K. Kasavajhala, K. A. A. Belfon, L. Raguette, H. Huang, A. N. Migues, J. Bickel, Y. Wang, J. Pincay, Q. Wu, C. Simmerling, *J. Chem. Theory Comput.* **2020**, *16*, 528–552.

[62] J. Wang, R. M. Wolf, J. W. Caldwell, P. A. Kollman, D. A. Case, *J. Comput. Chem.* **2004**, *25*, 1157–1174.